## CONDENSED MATTER

# Photoinduced Nonlinear Dynamics of Strongly Correlated Systems with Spin Crossover: Autocatalytic Spin Transition

**Yu. S. Orlov[a,b,\*], S. V. Nikolaev[a,b], and N. N. Paklin[a]**

*[a] Siberian Federal University, Krasnoyarsk, 660041 Russia*

*[b] Kirensky Institute of Physics, Federal Research Center KSC, Siberian Branch, Russian Academy of Sciences, Krasnoyarsk, 660036 Russia*

*\*e-mail: jso.krasn@mail.ru*

Nonlinear phenomena similar to the Belousov–Zhabotinsky reaction (autocatalytic oscillations of the population of high-spin and low-spin multielectron states of a transition metal ion) in open systems with spin crossover near bistability are considered. The conditions for possible experimental observation of autocatalytic oscillations of the magnetization in magnetically ordered systems with spin crossover are analyzed.

**1.** Spin crossover systems include a wide class of substances such as organometallic complexes, organic radicals, inorganic salts, and transition metal oxides. Most of them have been studied for more than half a century, but they still attract the permanent attention of researchers from physics, chemistry, biology, and medicine primarily due to the development and emergence of new experimental capabilities, e.g., the creation of ultra-high magnetic fields and pressures, the development of pump–probe spectroscopy with high time resolution, and nanostructuring. Theoretical and experimental studies of nonlinear phenomena (including autocatalytic oscillations of the population of multielectron states of a transition metal ion similar to the Belousov–Zhabotinsky reaction) in open spin crossover systems were reported in [1−15]. Most of these studies deal with weakly magnetic organometallic complexes. The problem of the formation of spatiotemporal dissipative structures in magnetically ordered systems (transition metal oxides [16]) near spin bistability has not yet been discussed in the literature and remains open. The main innovation of such systems is that the spontaneous formation of dissipative structures in them is due not to the true diffusion of matter (as in the observation of Turing structures in hydrodynamics or biology), but to the effective diffusion of densities of low-spin (LS) and high-spin (HS) multielectron states. In this work, formation mechanisms of such spatiotemporal structures under highly nonequilibrium conditions are theoretically simulated. These spatiotemporal structures correspond to a supramolecular coherent behavior of a huge number of transition metal ions, in which temporal and spatial oscillations of the macroscopic population of mul-

tielectron terms with different multiplicities and magnetization are possible.

**2.** We consider the specific case of $S_{HS} = 2$ and $S_{LS} = 0$, which corresponds to the $3d^6$ electron configuration of a transition metal ion (e.g., FeO, $(Mg_{1-x}Fe_x)O$). To describe cooperative phenomena (interactions) in spin crossover systems, we use the effective Hamiltonian [17, 18]

$$\hat{H} = -\frac{1}{2}J_\tau \sum_{\langle i,j \rangle} \hat{\tau}_i^z \cdot \hat{\tau}_j^z$$
$$+\frac{1}{2}(\varepsilon_S - k_B T \ln g)\sum_i \hat{\tau}_i^z + \frac{1}{2}J_S \sum_{\langle i,j \rangle} \hat{\mathbf{S}}_i \cdot \hat{\mathbf{S}}_j. \tag{1}$$

Here, the first term, written in the representation of the pseudospin vector operator $\hat{\boldsymbol{\tau}}$, describes the elastic ion−ion interaction, which is microscopically due to the electron−phonon interaction; $\hat{\tau}^z$ is the pseudospin projection operator having two eigenvalues $\tau^z = +1$ and $-1$ corresponding to the HS and LS states, respectively; and $J_\tau$ is the elastic interaction parameter. The ionic radii of cations in the LS and HS states differ quite strongly (by about 10%); in addition, the electronic−vibrational (vibronic) interaction leads to the dependence of the metal−ligand bond length on the electronic HS/LS state [19] (a spin transition LS → HS leads to an increase in the volume of the coordination complex); therefore, ferromagnetic (FM) pseudospin ordering is more energy-favorable. The second term in Eq. (1) contains the single-ion energy of multielectron states in the crystal field. A spin gap $\varepsilon_S = E_{HS} - E_{LS}$ is the difference between the energies of the HS and LS terms and depends on the
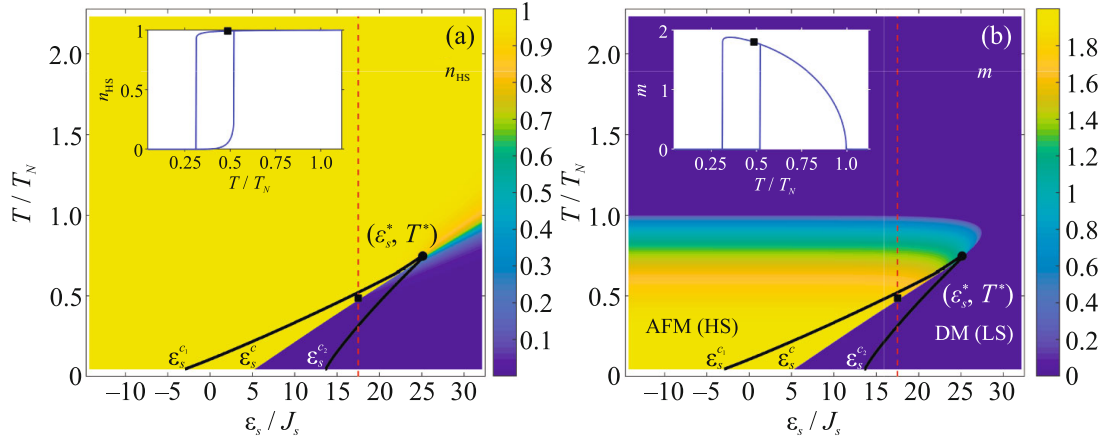
**Fig. 1.** (Color online) Calculated phase diagrams of the (a) population of the HS state $n_{HS}$ and (b) magnetization $m$. Insets show the temperature dependences of (a) $n_{HS}$ and (b) $m$ at $\varepsilon_S = 17.5 J_S$ marked by the vertical red dashed line. The calculations were performed at $z = 4$; $J_S = 28$ K [20], and $g = 1100$, $J_\tau = 38$ K [1]. In the point ($\varepsilon_S = 17.5 J_S$, $T = T_0 = 0.48 T_N$) marked by the square and used below as the initial one (a) $n_{HS} = n_{HS,0} = 0.99$, (b) $m = m_0 = 1.8$.

crystal field $10Dq = \Delta$. Without all cooperative interactions, the ground state is the HS state at $\varepsilon_S < 0$ (weak crystal field, $\Delta < \Delta_C$) and is the LS state at $\varepsilon_S > 0$ (strong crystal field, $\Delta > \Delta_C$). In the crossover point, $\varepsilon_S = \varepsilon_C = 0$. The critical value $\Delta_C$ is determined by the intraionic Hund interaction. In Eq. (1), $g = g_{HS}/g_{LS}$, where $g_{HS}$ and $g_{LS}$ are the degeneracies of the HS and LS states, respectively. Since the pseudospin projection operator has only two eigenvalues, to take into account the different degeneracies of the HS and LS states, the second term in Eq. (1) contains a temperature-dependent contribution. The third term in Eq. (1) describes the interatomic exchange interaction with the parameter $J_S$.

**3.** Since most transition metal oxides exhibit antiferromagnetic (AFM) spin ordering at normal pressure, the Hamiltonian (1) in the mean field (MF) approximation takes the form (FM for a pseudospin, AFM for a spin)

$$\hat{H}_{MF} = D_\tau \sum_i \hat{\tau}_i^z + D_S \sum_i \hat{S}_i^z + H_0. \quad (2)$$

Here, $D_\tau = \Delta_{eff} - z J_\tau \tau$, where $\Delta_{eff} = \frac{1}{2}(\varepsilon_S - k_B T \ln g)$, $z$ is the number of nearest neighbors, and $\tau = \langle \hat{\tau}^z \rangle$ (here and below, angle brackets $\langle ... \rangle$ denote the thermodynamic average); $D_S = z J_S m$, where $m = \langle \hat{S}^z \rangle$ is the sublattice magnetization; and $H_0 = \frac{1}{2} z J_\tau N \tau^2 + \frac{1}{2} z J_S N m^2$.

Solving the eigenvalue problem

$$\hat{H}_{MF} |\psi_k\rangle = E_k |\psi_k\rangle, \quad (3)$$

where $|\psi_k\rangle = C_{LS} |LS\rangle + C_{HS} |HS\rangle$ are the eigenstates of the Hamiltonian $\hat{H}_{MF}$, and using solutions that correspond to the minimum of the free energy $F = -k_B T \ln Z$, where

$$Z = e^{-\beta H_0} \left( e^{\beta D_\tau} + e^{-\beta D_\tau} \frac{\sinh\left[\left(S + \frac{1}{2}\right)\beta D_S\right]}{\sinh(\beta D_S / 2)} \right) \quad (4)$$

is the partition function, where $\beta = 1/(k_B T)$, it is possible to calculate the thermodynamic averages included in $\hat{H}_{MF}$:

$$m = \frac{1}{Z} \sum_k \langle \psi_k | \hat{S}^z | \psi_k \rangle e^{-E_k \beta},$$

$$\tau = \frac{1}{Z} \sum_k \langle \psi_k | \hat{\tau}^z | \psi_k \rangle e^{-E_k \beta}.$$

Thus, when solving Eq. (3), we deal with the self-consistent problem of finding the eigenstates and eigenvalues of the effective Hamiltonian in the mean field approximation.

Figure 1 shows the calculated (spin gap $\varepsilon_S$, temperature $T$) phase diagrams of (a) the population of the HS state $n_{HS} = \frac{\tau + 1}{2}$ and (b) the magnetization $m$. Here and below, the temperature and the spin gap are given in units of the Néel temperature $T_N = z J_S \frac{S(S+1)}{3}$ and of the exchange integral $J_S$, respectively. It can be seen that because of the cooperative interaction $J_S$, the system retains its HS ground state up to $\varepsilon_S = \varepsilon_S^C \approx 5 J_S$, although according to the single-ion theory, the system at $\varepsilon_S > 0$ should have the LS

ground state. The increase in the critical value $\varepsilon_S^C$ caused by cooperative effects is quite understandable since the exchange interaction $J_S$ stabilizes the HS state, lowering its energy. The AFM (HS) ground state is replaced by the diamagnetic LS state, DM (LS), at $\varepsilon_S > \varepsilon_S^C$ (see Fig. 1b). The elastic interaction $J_\tau$ unlike the exchange one $J_S$ does not increase $\varepsilon_S^C$, but it, as well as $J_S$, transforms smooth spin crossover into a first-order phase transition at low temperatures.

The diagrams presented in Fig. 1 indicate the existence of a singular point: a tricritical point $(\varepsilon_S^*, T^*)$, in which the line of the second-order phase transition continuously transforms into the line of the first-order phase transition. In Fig. 1, black solid lines show the region of metastable states. Insets of Fig. 1 present sections along the red dashed line.

**4.** We consider now the spin crossover system thermally coupled to a reservoir (thermostat) with the temperature $T_R$ and in the external radiation field with the intensity $I_0$, leading to photothermal heating of the system. The variation of its temperature $T$ in time $t$ can be set by the equation

$$\frac{\partial T}{\partial t} = -\alpha(T - T_R) + I\left(1 + (\rho_0 - 1)\frac{\tau + 1}{2}\right) \\ -\frac{\Delta H_\tau}{C_p}\frac{\partial \tau}{\partial t} - \frac{\Delta H_S}{C_p}\frac{\partial m}{\partial t}. \tag{5}$$

Here, the first term on the right-hand side describes coupling to the thermostat ($\alpha$ is the coupling coefficient). The second term is due to the absorption of external radiation $I = I_0 \dfrac{a_{LS} M}{C_p m_a}$, where $a_{LS}$ is the absorption coefficient in the LS state, $M$ is the molar mass, $C_p$ is the molar heat capacity, and $m_a$ is the sample mass, and $\rho_0 = a_{HS}/a_{LS}$, where $a_{HS}$ is the absorption coefficient in the HS state. The last two terms determine the change in the temperature under the variation of the enthalpy $\Delta H = \Delta H_\tau + \Delta H_S = T_{eq}\Delta S$ due to the spin transition, where $\Delta H_\tau$ and $\Delta H_S$ are changes in the orbital and spin enthalpies, $T_{eq} = \dfrac{\varepsilon_S}{k_B \ln g}$ is the temperature, at which $n_{HS} = n_{LS}$, and $\Delta S = R \ln g$ is a change in the entropy (here, $R$ is the gas constant).

In a nonequilibrium state, the change in the magnetization $m$ and thermodynamic average $\tau$ can be described using the relaxation equation

$$\frac{\partial \xi}{\partial t} = -\Gamma_\xi \frac{\partial F}{\partial \xi}, \tag{6}$$

where $\xi = m, \tau$. Taking into account Eq. (4), we obtain

$$\frac{\partial m}{\partial t} = -z\Gamma_S J_S\left(m + e^{-\beta D_\tau} S B_S(\beta S D_S)\frac{\sinh\left[\left(S + \frac{1}{2}\right)\beta D_S\right]}{e^{\beta D_\tau}\sinh(\beta D_S/2) + e^{-\beta D_\tau}\sinh\left[\left(S + \frac{1}{2}\right)\beta D_S\right]}\right), \tag{7}$$

$$\frac{\partial \tau}{\partial t} = -z\Gamma_\tau J_\tau\left(\tau + \frac{e^{\beta D_\tau}\sinh(\beta D_S/2) - e^{-\beta D_\tau}\sinh\left[\left(S + \frac{1}{2}\right)\beta D_S\right]}{e^{\beta D_\tau}\sinh(\beta D_S/2) + e^{-\beta D_\tau}\sinh\left[\left(S + \frac{1}{2}\right)\beta D_S\right]}\right), \tag{8}$$

where

$$B_S(\beta S D_S) \\ = \frac{(2S + 1)}{2S}\coth\left[\frac{(2S + 1)}{2S}\beta S D_S\right] - \frac{1}{2S}\coth\left(\frac{1}{2S}\beta S D_S\right)$$

is the Brillouin function.

Equations (5), (7), and (8) are macroscopic for thermodynamic averages and are derived by neglecting all time correlation functions. This consideration is justified if thermodynamic equilibrium is established in a time much shorter than the characteristic times of change in the parameters $m$, $n_{HS}$, and $T$. Otherwise, it is necessary to consider the dynamics of quantum states directly. As we see below, the characteristic period $T_A$ of autocatalytic oscillations is from tenths to

units of a second (depending on the parameters used and initial conditions), which is much larger than the characteristic times of spin–lattice relaxation, spin–orbit or exchange interaction, magnetic precession, and any other processes of the change in the magnetization in the medium occurring in picoseconds [21–23]. At the same time, the characteristic HS $\leftrightarrow$ LS relaxation time in spin crossover systems depends strongly on the compound under consideration, but it is nanoseconds in most cases, and the photothermal heating time corresponds to the microsecond scale [24].

Figure 2 shows the result of solving the system of equations (5), (7), and (8) at $T_R = 35$ K, $\varepsilon_S = 17.5 J_S$ (shown by the red dashed line in Fig. 1), $I = 800$ K/s, and the parameters $\Gamma_S = 5 \times 10^{-2}$ K$^{-1}$ s$^{-1}$, $\Gamma_\tau = 5 \times$
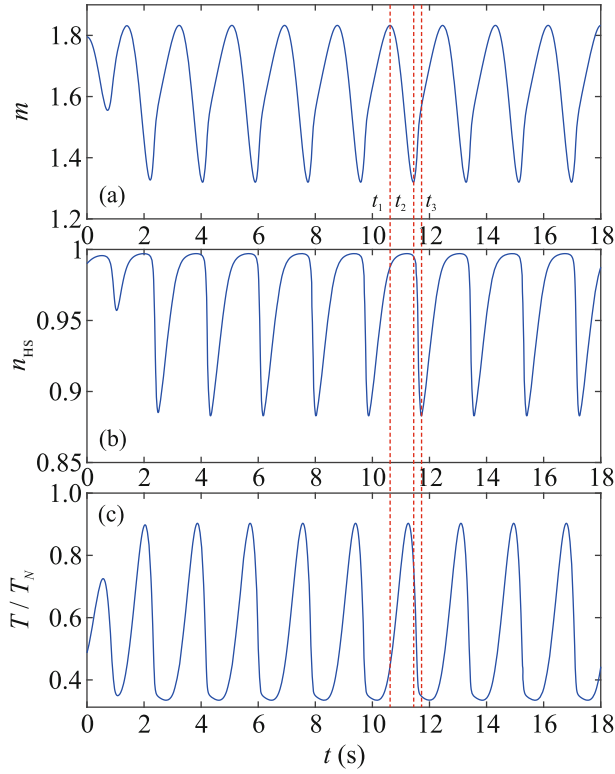
**Fig. 2.** (Color online) Time dependence of the (a) magnetization $m$, (b) population of the multielectron HS state $n_{HS}$, and (c) sample temperature $T$, obtained from the numerical solution of the system of equations (5), (7), and (8) under initial conditions $m_0 = 1.8$, $n_{HS,0} = 0.99$, and $T_0 = 0.48 T_N$, corresponding to the thermodynamic equilibrium state marked by the square in Fig. 1. Vertical dashed lines are drawn for ease of comparison and correspond to times $t_1$, $t_2$, and $t_3$.

$10^{-1}$ $K^{-1}$ $s^{-1}$, $\alpha = 7$ $s^{-1}$, $a_{LS} = 0.4$, $a_{HS} = 0.3$, $\Delta H_S / C_P = 636$ K, and $\Delta H_\tau / C_P = 320$ K taken from [1], where their analysis and evaluation from experimental data are given. It can be seen that a stationary mode of autocatalytic oscillations of the magnetization $m$, the population of the multielectron HS state $n_{HS}$, and the sample temperature $T$ is established in an open nonequilibrium system (see Fig. 2). Of all three characteristics, the magnetization is the least inert and responds almost instantly to changes in the population and temperature. In the time interval from $t_1$ to $t_2$ (see Fig. 2a), $m$ decreases, while $n_{HS}$ hardly changes; i.e., the population is redistributed between HS sublevels with different spin projections due to the variation of the temperature. In the interval from $t_2$ to $t_3$, $n_{HS}$ decreases sharply along with $T$, but remains above the percolation threshold, so the magnetization increases. The increase in the magnetization continues in the range from $t_3$ to $t_1 + T_A$ although the temperature in this range barely changes, but $n_{HS}$ increases. Thus,

there are two mechanisms for the change in the magnetization: (i) the redistribution between HS states with different projections and (ii) the change in the ratio between HS and LS states.

The physical mechanism of oscillations in the populations of spin states (terms with different multiplicities), the magnetization, and the temperature can be understood as follows. In the time interval from $t_1$ to $t_2$, the population $n_{HS}$ (see Fig. 2b) is close to unity and barely changes over time. Since $a_{HS} < a_{LS}$, the system gets the least energy from external radiation during this time interval. The temperature and the population decrease sharply in the time range from $t_2$ to $t_3$ due to the coupling to the reservoir ($T_R = 35$ K $\approx 0.16 T_N$) (see Figs. 2b and 2c). The decrease in the temperature below the equilibrium value $T_0 = 0.48 T_N$ (marked by the square in Fig. 1 and used as the initial value for solving the system of equations (5), (7), and (8)) leads to an increase in the magnetization (despite the decrease, $n_{HS}$ remains above the leakage threshold). In the time range from $t_3$ to $t_1 + T_A$, the temperature barely changes and remains below the equilibrium value $T_0$ (see Fig. 2c), which leads to an increase in the magnetization (see Fig. 2a). In turn, the increase in the magnetization due to the cooperative exchange interaction $J_S$ increases the population $n_{HS}$ (see Fig. 2b), which tends to its equilibrium value $n_{HS,0} = 0.99$ (the initial value marked with a square in Fig. 1). The decrease in $n_{HS}$ (the increase in $n_{LS} = 1 - n_{HS}$) increases the absorption of external radiation and, as a consequence, the temperature after the time $t_3$. In turn, a temperature increase reduces the magnetization after the time $t_1$. The process is then repeated.

Autocatalytic oscillations are possible near bistability, when there is a boundary between the region of overheated and overcooled metastable states on both sides of a first-order phase transition. In our case, they take place at $\varepsilon_S^{C_2} < \varepsilon_S < \varepsilon_S^*$ (see Fig. 1). There is only one (upper temperature) boundary at $\varepsilon_S^{C_1} < \varepsilon_S < \varepsilon_S^{C_2}$ (see Fig. 1); therefore, autocatalytic oscillations become impossible in this case.

In addition to the solutions shown in Fig. 2, there is another type of solutions where the magnetization vanishes, but autocatalytic oscillations of $n_{HS}$ and $T$ remain (see Fig. 3). The differences are due to the choice of other initial conditions: $m_0 = 1.5$, $n_{HS,0} = 0.5$, $T_0 = 0.36 T_N$, and parameters: $a_{HS} = 0.13$, $\Delta H_S / C_P = 97$ K, $\Delta H_\tau / C_P = 5$ K (the $a_{LS}$, $\Gamma_S$, $\Gamma_\tau$, and $\alpha$ values remained the same). Figure 3 shows that undamped oscillations of $n_{HS}$ can coexist with damped oscillations of $m$, which is associated with two possible mechanisms of magnetization changes described above. The calculation results show that the oscilla-
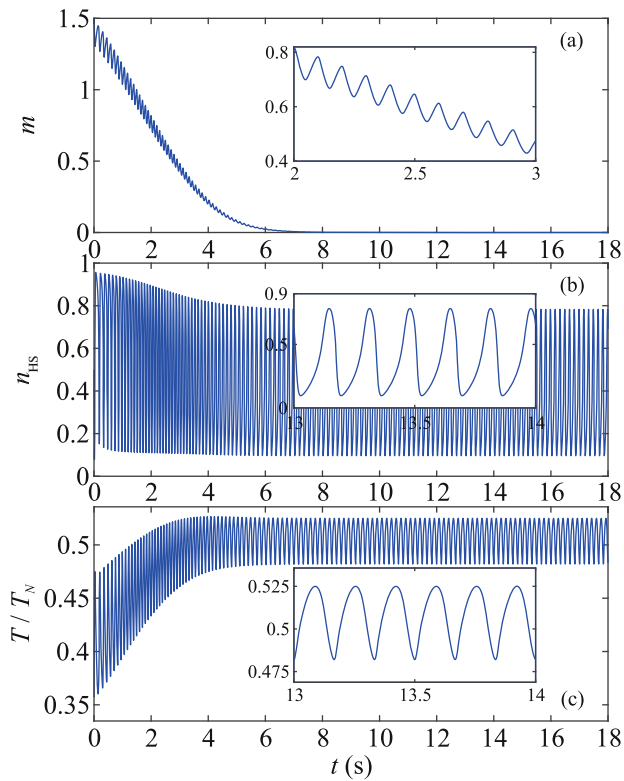
**Fig. 3.** (Color online) Time dependence of the (a) magnetization $m$, (b) population $n_{HS}$ of the multielectron HS state, and (c) sample temperature $T$, obtained from the numerical solution of the system of equations (5), (7), and (8) under the initial conditions $m_0 = 1.5$, $n_{HS,0} = 0.5$, and $T_0 = 0.36T_N$. The insets show the dependences on an enlarged scale.



**Fig. 4.** (Color online) Trajectory of the system in the phase space $m$, $n_{HS}$, and $T$ for cases shown in Figs. 2a and 3b.

tions of $n_{HS}$, which were studied disregarding the magnetic subsystem under similar parameters in [1], do not yet mean the corresponding autocatalytic oscillations of the magnetization, which should be taken into account to prepare the experiment.

Figures 4a and 4b show the trajectory of the system in the phase space of the parameters $m$, $n_{HS}$, and $T$ for cases shown in Figs. 2 and 3, respectively. It can be seen that the trajectory for the first type of solutions (see Fig. 2) approaches the limit cycle (see Fig. 4a), and the limit cycle for the second type (see Fig. 3) lies in the plane $m = 0$ (see Fig. 4b).

**5.** Thus, the nonlinearity (which is ensured by bistability) and positive feedback given by the last three terms on the right-hand side of Eq. (5) are necessary for the formation of autocatalytic oscillations. It is important to note that a system with autocatalytic reactions of the Belousov−Zhabotinsky type involves nonlinear mechanisms that ensure a periodic transition from one state to another. In this work, nonlinear equations have a completely different form. It is the feedback that leads to instability and the resulting

oscillations, which, however, do not arise without external radiation responsible for thermal heating and a nonzero rate of the change in $m$ and $n_{HS}$. In our case, the process can be called autocatalytic if it is self-accelerating or self-sustaining.

Due to the strong coupling of electron, magnetic and structural degrees of freedom, the phenomenon of spin crossover is associated with a fairly strong change in the volume $V$ of a crystal lattice. Along with the regular component of the thermal expansion coefficient due to the anharmonicity of lattice vibrations, there is an anomalous contribution from the vibronic interaction [19]. Therefore, in a more general case, Eqs. (5), (7), and (8) should be supplemented with the equation of motion for $V$. The inclusion of the change in the volume can somehow affect the formation of magnetization oscillations in magnetically ordered systems with spin crossover due to the magnetostriction effect and make its physical content richer. Using the Birch−Murnaghan equation, one can directly relate the change in $V$ to the population $n_{HS}$ [25]. However, due to the smallness of magnetostriction in the substances under consideration, the inclusion of a change in the volume hardly changes the results obtained.

## CONFLICT OF INTEREST

The authors of this work declare that they have no conflicts of interest.

## REFERENCES

1. K. Boukheddaden, M. Paez-Espejo, F. Varret, and M. Sy, Phys. Rev. B **89**, 224303 (2014).

2. F. Varret, M. Paez-Espejo, and K. Boukheddaden, Europhys. Lett. **104**, 27003 (2013).

3. A. Slimani, F. Varret, K. Boukheddaden, D. Garrot, H. Oubouchou, and S. Kaizaki, Phys. Rev. Lett. **110**, 087208 (2013).

4. M. Sy, F. Varret, K. Boukheddaden, G. Bouchez, J. Marrot, S. Kawata, and S. Kaizaki, Angew. Chem. Int. Ed. **53**, 7539 (2014).

5. M. Paez-Espejo, M. Sy, F. Varret, and K. Boukheddaden, Phys. Rev. B **89**, 024306 (2014).

6. M. Sy, D. Garrot, A. Slimani, M. Paez-Espejo, F. Varret, and K. Boukheddaden, Angew. Chem. Int. Ed. **55**, 1755 (2016).

7. T. Nishihara, A. Bousseksou, and K. Tanaka, Opt. Express **21**, 31179 (2013).

8. K. Boukheddaden, M. Sy, and F. Varret, Adv. Theory Simul. **1**, 1800080 (2018).

9. M. Sy and K. Boukheddaden, J. Phys. Chem. C **124**, 28093 (2020).

10. Y. Singh, K. Affes, N.-I. Belmouri, and K. Boukheddaden, Mater. Today Phys. **27**, 100842 (2022).

11. M. Ndiaye, Y. Singh, H. Fourati, M. Sy, B. Lo, and K. Boukheddaden, J. Appl. Phys. **129**, 153901 (2021).

12. H. Fourati, M. Ndiaye, M. Sy, S. Triki, G. Chastanet, S. Pillet, and K. Boukheddaden, Phys. Rev. B **105**, 174436 (2022).

13. K. Boukheddaden, H. Fourati, Y. Singh, and G. Chastanet, Magnetochemistry **5** (2), 21 (2019).

14. M. Sy, R. Traiche, H. Fourati, Y. Singh, F. Varret, and K. Boukheddaden, J. Phys. Chem. C **122**, 20952 (2018).

15. H. Fourati, G. Bouchez, M. Paez-Espejo, S. Triki, and K. Boukheddaden, Crystals **9**, 46 (2019).

16. I. S. Lyubutin and A. G. Gavriliuk, Phys. Usp. **52**, 989 (2009).

17. K. Boukheddaden, I. Shteto, B. Hoo, and F. Varret, Phys. Rev. B **62**, 14796 (2000).

18. J. Nasu, T. Watanabe, M. Naka, and S. Ishihara, Rev. B **93**, 205136 (2016).

19. Y. S. Orlov, V. A. Dudnikov, A. E. Sokolov, T. M. Ovchinnikova, N. P. Shestakov, and S. G. Ovchinnikov, JETP Lett. **115**, 615 (2022).

20. M. J. R. Hoch, S. Nellutla, J. van Tol, E. S. Choi, J. Lu, H. Zheng, and J. F. Mitchell, Phys. Rev. B **79**, 214421 (2009).

21. A. Kirilyuk, A. V. Kimel, and T. Rasing, Rev. Mod. Phys. **82**, 2731 (2010).

22. A. M. Kalashnikova, A. V. Kimel, and R. V. Pisarev, Phys. Usp. **58**, 969 (2015).

23. A. V. Kimel, A. Kirilyuk, P. A. Usachev, R. V. Pisarev, A. M. Balbashov, and Th. Rasing, Nature (London, U.K.) **435**, 655 (2005).

24. E. Collet and P. Guionneau, C. R. Chim. **21**, 1133 (2018).

25. Y. S. Orlov, S. V. Nikolaev, A. I. Nesterov, and S. G. Ovchinnikov, JETP Lett. **105**, 771 (2017).

*Translated by L. Mosina*